J. Plasma Physics (2006), *vol.* 72, *part* 5, *pp.* 671–686.
doi:10.1017/S002237780500423X First published online 8 March 2006 Printed in the United Kingdom

Stability analysis of nonlinear evolution patterns of modulational instability and chaos using one-dimensional Zakharov equations

K. BATRA[1], R.P. SHARMA[1] and A.D. VERGA[2]

[1]Centre for Energy Studies, Indian Institute of Technology, New Delhi—110016, India (karunab2004@hotmail.com)

[2]Institut de recherché sur les phénomènes hors équilibre 49, rue F. Joliot-Curie, BP 146, 13384 Marseille cedex 13, France

(Received 16 May 2005 and accepted 20 October 2005)

Abstract. In the present paper the long-term behavior of the nonlinear dynamical evolution of modulational instability is investigated by using a simplified model for one-dimensional Zakharov equations, which couples the electrostatic electron plasma wave and ion-acoustic wave propagation. The manuscript details on the occurrence of fixed points and fixed-point attractors for a suitable value of the wavenumber of perturbation through associated bifurcations, both for the adiabatic (nonlinear Schrödinger equation) and non-adiabatic cases for Zakharov equations. It is shown that these evolutions are quite sensitive to initial conditions, Fermi–Pasta–Ulam recurrence is broken up and a chaotic state develops for the non-adiabatic case. Regular patterns with a periodic sequence in space and time and spatiotemporal chaos with irregular localized patterns are formed in different regions of unstable wavenumbers, hence producing a self-organizing dynamical system. The results are consistent with those obtained by numerically solving Zakharov equations as previously reported and summarized in the present manuscript.

1. Introduction

In various branches of physics there is an interest in the stability of (simple) solutions of nonlinear problems. These solutions, which are usually equilibria of the related physical system, are in many cases found to be unstable to infinitesimal perturbations. The question then arises as to whether the physical system can evolve from unstable (relatively simple) equilibrium to a more complicated equilibrium (limit cycle behavior). If dissipation is present, limit cycle behavior seems likely to occur because the tendency towards a new equilibrium is accompanied by an increase in the entropy of the system. However, when dissipation is absent, it is not at all obvious that the limit cycle behavior occurs. After reaching maximum amplitude the unstable mode decreases in amplitude and eventually returns to its initial value and this process is repeated in time. This long-term, periodic behavior of the nonlinear system has become known as the Fermi–Pasta–Ulam (FPU) recurrence phenomenon.

Extensive research has been done to study the above phenomenon where the nonlinear Schrödinger (NLS) equation is considered as the basic envelope equation of a dispersive wave system that is weakly nonlinear and has also found numerous applications in plasma physics, in the theoretical study of deep water waves [1, 2] and also as a model for nonlinear pulse propagation in fibers [3]. The Zakharov equations

$$i\frac{\partial E}{\partial t} + \frac{\partial^2 E}{\partial x^2} = nE, \tag{1a}$$

$$\frac{\partial^2 n}{\partial t^2} - \frac{\partial^2 n}{\partial x^2} = \frac{\partial^2}{\partial x^2}|E|^2, \tag{1b}$$

where $E(x,t)$ is the dimensionless slowly varying (in time) envelope of the high-frequency electric field, $n(x,t)$ is the dimensionless low-frequency density fluctuation associated with the ion-acoustic field, t is the dimensionless time and x is the dimensionless distance, are (along with their extended forms) also used as model equations in the study of ionospheric heating by radiowaves in the F layer for the study of Langmuir turbulence [4], resonant absorption of laser beams near the critical density region [5,6] and stimulated Raman and Brillouin scattering in a laser plasma interaction in a fully nonlinear stage as investigated in [7]. In plasmas, the NLS equation describes the modulational instability (MI) of the monochromatic Langmuir waves [1, 8–11]. For initial conditions that decay sufficiently with large distances, the NLS equation is integrable by the inverse scattering transform and admits asymptotically a finite number of stable solitons [12, 13]. For spatially periodic (in space) fields the numerical results of Yuen and Fergusen [2] have predicted FPU recurrence. Infield [8] has also developed a model to explain this recurrence by taking the first few harmonics and predicting that the actual amplitude of the harmonics is less than that predicted by the numerical simulation of Yuen and Fergusen [2]. Moreover, two patterns of development exist for the NLS, which has been investigated numerically by Moon [9]. Goldstein and Rozmus [10] have constructed a model for the nonlinear evolution of modulation instability using the Ritz variational method to predict the development of instability through the localization to a quasi-soliton state and a periodic recurrence of the initial condition. Similar methods have also been used to investigate the evolution of Gaussian-shaped pulses connected with the Zakharov equations by Bhakta [14]. Tracy and Chen [11] dealt with the so-called N-phase wavetrain solutions of the cubic Schrödinger equation and discussed the recurrence phenomena for systems with a finite spatial period as well as developing a method for calculating the recurrence time.

The NLS equation, which is the adiabatic limit of the Zakharov equations coupling the electrostatic plasma wave and ion-acoustic wave propagation [12,13], is not able to give a complete picture of the nonlinear saturation mechanism. The effect of relaxing the condition of adiabaticity may modify the nonlinear evolution of the modulational instability and the FPU recurrences. Moreover, spatiotemporal chaos in a continuum Hamiltonian system is an important subject used to investigate the long-term behavior of a volume preserving system with an infinite number of degrees of freedom, which leads to a solitary pattern.

In this paper we continue our interest in extensively modeled examples of recurrence, namely, in the modulational instability (also known as the Benjamin–Feir instability, or side-band instability), using one-dimensional (1D) Zakharov

equations, which are one of the most extensively studied models used to describe strong turbulence in plasmas. We develop a simplified model that is used to explain the temporal features of the evolution pattern as predicted numerically using the 1D Zakharov equations. This model not only establishes the fact that as the condition of adiabaticity is relaxed and the recurrence disappears but also that the existence of a chaotic state can be established. Furthermore, this paper also reports on the stability of the system through associated equilibrium points and bifurcations analytically, using the simplified model. A fixed-point analysis of the system using the simplified model indicates the presence of a fixed-point attractor at the same value of wavenumber of perturbation where complete FPU recurrence is obtained numerically. Results are consistent with those obtained numerically as also from using the Zakharov model.

In Sec. 2 we derive dynamical equations for the simplified model. In Sec. 3, we compare the computer simulation results from the simplified model for the non-adiabatic case with those obtained by solving 1D Zakharov equations numerically. Section 4 gives a detailed stability analysis of the model with the help of various simulations and discusses the conditions of stability with associated fixed points and attractors for the non-adiabatic and the adiabatic case for a specific value of the wavenumber of perturbation. We present concluding remarks in Sec. 5.

2. Simplified model equations

In order to study the stability of the field envelope to infinitesimal perturbations we describe the general solution as a superposition of a set of normal modes as

$$E = E_0(t) + E_{-1}(t)e^{-i\alpha x} + E_1(t)e^{i\alpha x}, \tag{2}$$

where

$$E_{-1}(0) = E_1(0)$$

and

$$n = n_0 + (n_1(t)e^{i\alpha x} + n_2(t)e^{2i\alpha x} + c.c.). \tag{3}$$

Similar methods have been used in fluid dynamics by Benney [15] where it was shown that if the amplitudes of the three primary waves are regarded as slowly varying functions of time, rather than as strict constants, the interactions can be described by much simplified equations that are apparently valid even when the amplitude in the fourth mode becomes comparable with that in the other three. Complete solutions of Benney's equations, which are periodic functions of time, were obtained by Bretherton [16]. Rowlands and Janssen [17] independently used the fact that, for a wavenumber sufficiently near the critical value, calculations to study the FPU recurrence in the NLS equation can be somewhat simplified. They obtained the long-term behavior of the modulation of the linearly unstable mode in this limit, leading to a qualitative confirmation of the numerical results of Yuen and Fergusen [2]. A more general calculation using similar methods in which the wavenumber is not restricted for the NLS equation was given by Infield [8].

Substituting the above expressions in (1a) and on comparing coefficients we obtain the following three equations,

$$i\dot{E}_0 = n_0E_0 + n_1E_{-1} + n_1^*E_1, \tag{4}$$

$$i\dot{E}_{-1} = \alpha^2E_{-1} + n_0E_{-1} + n_1^*E_0 + n_2^*E_1, \tag{5}$$

$$i\dot{E}_1 = \alpha^2E_1 + n_0E_1 + n_1E_0 + n_2E_{-1}. \tag{6}$$

https://doi.org/10.1017/S002237780500423X Published online by Cambridge University Press

Multiplying (4) by $\dot{E}_0^*$ and subtracting the complex conjugate of the resulting equation from itself gives

$$i|\dot{E_0}|^2 = n_1(E_{-1}E_0^* - E_1^*E_0) + n_1^*(E_1E_0^* - E_{-1}^*E_0). \tag{7}$$

Similarly on using (5) and (6) we obtain

$$i|\dot{E_{-1}}|^2 = n_1^*E_0E_{-1}^* + n_2^*E_1E_{-1}^* - n_1E_{-1}E_0^* - n_2E_1^*E_{-1} \tag{8}$$

and

$$i|\dot{E_1}|^2 = n_1E_0E_1^* + n_2E_{-1}E_1^* - n_1^*E_1E_0^* - n_2^*E_{-1}^*E_1. \tag{9}$$

Adding (7), (8) and (9) gives the following conservation equation consistent with the definition of the number of plasmons, N:

$$|E_0|^2 + |E_1|^2 + |E_{-1}|^2 = N. \tag{10}$$

We introduce the variables $\rho_0, \theta_0, \rho_1, \theta_1$ according to

$$E_0 = \rho_0 e^{i\theta_0}, \quad E_1 = E_{-1} = \rho_1 e^{i\theta_1} \tag{11}$$

and $\varphi = \theta_0^- \theta_1$ with $\rho_0 = \sqrt{n_0}\sin z$, $\rho_1 = \sqrt{n_0}/\sqrt{2}\cos z$, $a = 2z$.

Substituting (2) and (3) in (1b) with the assumption $n_1 = n_1^*$ and using (11) gives, on using $n_0 = N$,

$$\ddot{n}_1 + \alpha^2 n_1 = -\alpha^2 N \sin a \cos\varphi. \tag{12}$$

Furthermore,

$$\dot{a} = -4n_1 \sin\varphi \tag{13}$$

and

$$\dot{\varphi} = \alpha^2 - 2n_1 \cot a \cos\varphi. \tag{14}$$

Under the assumed equations (11), (2) and (3) can also be written as

$$E = \sqrt{N}\sin(a/2)e^{i\theta_0} + \sqrt{2N}\cos(a/2)e^{i\theta_1}\cos(\alpha x) = E_0 + 2\sqrt{2}E_1\cos\alpha x$$

and

$$n = N + n_1\cos(\alpha x). \tag{15}$$

When we assume the adiabaticity condition, the dynamical system can be written in Hamiltonian form as

$$\dot{\varphi} = \frac{\partial H}{\partial a} \tag{16}$$

and

$$\dot{a} = -\frac{\partial H}{\partial \varphi} \tag{17}$$

where

$$H = \alpha^2 a + N\sin a + N\sin a\cos 2\varphi. \tag{18}$$

3. Numerical solution to 1D Zakharov equations

We solve (1a) and (1b) numerically in a periodic box for the initial condition

$$E = A_0(1 + \beta e^{i\gamma}\cos\alpha x), \tag{19}$$

where A_0 is the amplitude of the pump Langmuir wave, β and γ are the parameters governing the magnitude and the phase of the perturbation while α is the

https://doi.org/10.1017/S002237780500423X Published online by Cambridge University Press

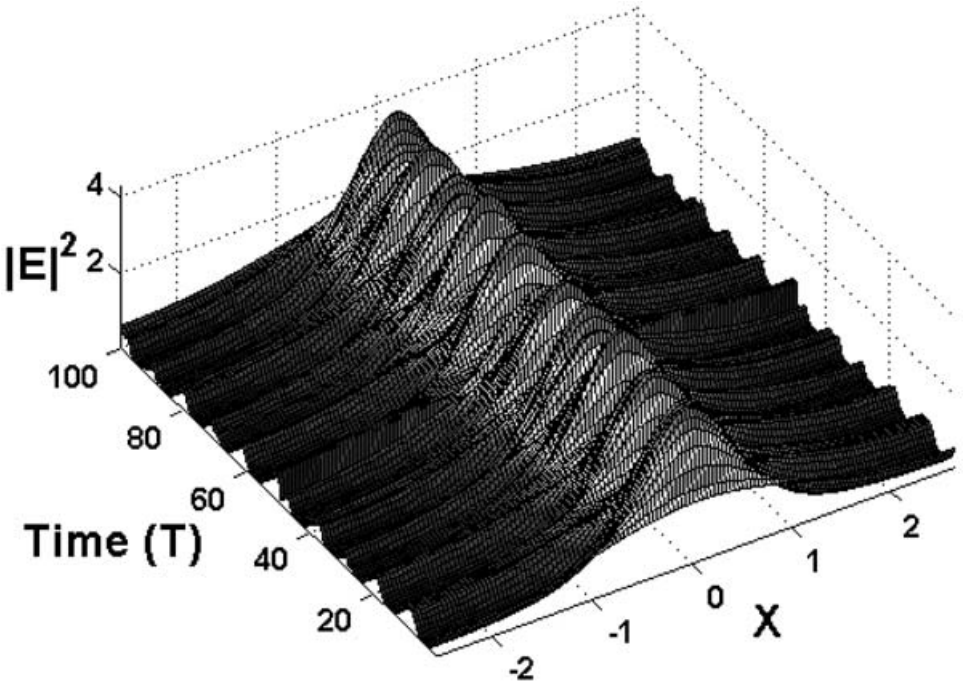

Figure 1. 3D field plot of the electric field for the Zakharov equations solved numerically for the initial condition (19) with $A_0 = 1$, $\beta = 0.1$, $\gamma = 0$ and $\alpha = 1.2$ showing no FPU recurrence as opposed to that obtained for the NLS case (see [9]).

wavenumber of the perturbation. This initial condition corresponds to a slightly perturbed plane Langmuir wave solution of the Zakharov equations. A pseudo-spectral method was used for space integration and a modified version of the Gazdag [18] predictor–corrector method was employed to investigate the evolution in time. The linear evolution is exactly integrated, forming an important feature of the code so as to accurately reproduce the instability, and a variable time step was used in order to monitor the invariants to the desired accuracy. Different evolution patterns are obtained with variations in the wavenumber of perturbation α. We have reported the patterns with their explanation in [19], giving details on the associated Lypaunov exponents describing the field trajectories. To compare the results of the simplified model with those obtained by numerically simulating the Zakharov equations we choose one typical case when $A_0 = 1$, $\beta = 0.1$, $\gamma = 0$ and $\alpha = 1.2$. The chosen parameter values correspond to the case where the NLS equation has the maximum growth rate for MI and also exhibits FPU recurrence. Figure 1 illustrates the three-dimensional (3D) spatio-temporal evolution of the electric field for the 1D Zakharov equations for the chosen parameter values.

It has already been reported by the authors in [19] that by suitably changing the wavenumber of perturbation, a Zakharov system can arrive at a periodic self-organized state exhibiting complete FPU recurrence. Bifurcations exist that separate the dynamical system from a chaotic to a periodic to a chaotic state. One such bifurcation point extensively studied by the authors numerically in [19] is at $\alpha = 1.39$. For reference, Fig. 2(a) is reproduced in this research paper depicting the 3D spatio-temporal evolution of the field profile for this value along with its

https://doi.org/10.1017/S002237780500423X Published online by Cambridge University Press

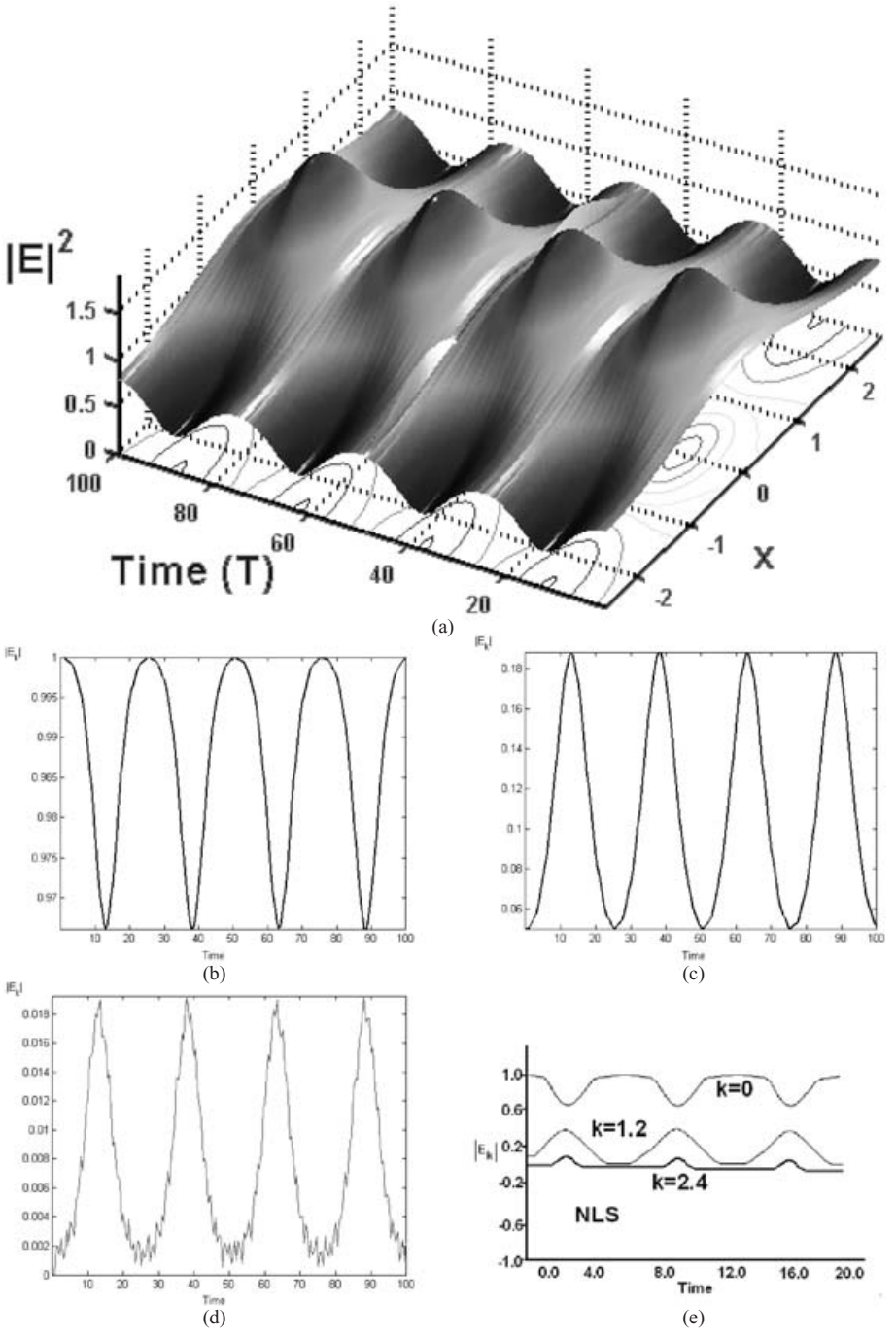

Figure 2. (a) 3D field plot of the electric field for the Zakharov equations solved numerically for the initial condition (19) with $A_0 = 1$, $\beta = 0.1$, $\gamma = 0$ and $\alpha = 1.39$ illustrating complete FPU recurrence. Time evolution of the absolute value of the Fourier component of the electric field for the Zakharov equations solved numerically for the initial condition (19) with $A_0 = 1$, $\beta = 0.1$, $\gamma = 0$ and $\alpha = 1.39$ (b) illustrating the maximum energy contained in the lowest order mode $k = 0$, (c) for $k = \alpha = 1.39$, (d) for $k = \alpha = 2.78$ and (e) for the first three harmonics.

https://doi.org/10.1017/S002237780500423X Published online by Cambridge University Press

contour plot. Complete periodicity (FPU recurrence) is obtained. Figures 2(b), 2(c) and 2(d) depict the time evolution of the absolute values of the Fourier components of the field for the first three harmonics illustrating that the energy in the system is confined to a few low modes, a characteristic feature of FPU recurrence. Similar behavior is also observed for the adiabatic case (NLS) [10]. Figure 2(e) reproduces the result for the adiabatic case.

Comparing (15) from the simplified model with the initial condition (19) allows us to define the following initial conditions (the subscript 0 identifies initial values of the parameters) for the solution of the simplified model:

$$z_0 = \arctan\left(\frac{\sqrt{2}}{\beta}\right), \quad \varphi_0 = -\gamma = 0, \quad \text{Plasmon number},$$

$$N = A_0^2\left(1 + \frac{\beta^2}{2}\right), \quad n_{10} = -N \sin 2z_0 \cos\varphi_0.$$

4. Nonlinear analysis of the system

4.1. Non-adiabatic case

In the non-adiabatic case, the simplified model (12)–(14) has been used to study the evolution of the electric field and density. Preliminary results comparing the results from the Zakharov model and the simplified model for the adiabatic case have been reported by the authors in [19]. However, we find that the simplified model can predict not only the existence of chaos but can also be used for in-depth analysis to investigate variation from a chaotic to a self-organized state through a careful numerical simulation of associated bifurcations. The wavenumber of perturbation $\alpha = 1.2$, which corresponds to the maximum growth rate of MI for the NLS case, depicting complete FPU recurrence, illustrates a completely chaotic behavior for the non-adiabatic case (Fig. 3) through the simplified model. Figure 4 for $\alpha = 1.41$ depicts a fixed-point attractor that draws the system to a single point in phase space for the non-adiabatic case, obtained through the simplified model and also through the Zakharov model (within the limits of numerical accuracy) consistent with the behavior depicted in Fig. 2(a) for $\alpha = 1.39$ through the numerical Zakharov model. Also note that the restricting volume in phase space attributed to constant φ values up to third decimal and in a values up to second decimal, a characteristic feature of self-organization. We report that $\alpha = 1.4$ (up to the first decimal place) is indeed a point of bifurcation, separating the dynamical system into two distinct dynamical behaviors. The behavior is highly sensitive to initial conditions as illustrated in Figs 5(a), 5(b) and 5(c) with minor variations in the initial amplitude, wavenumber and amplitude of perturbation, a behavior characteristic of nonlinear self-organizing dynamical systems.

For the evaluation of fixed points, $\dot{a} = 0$ from (13) implies $\varphi = n\pi$ which when used with $\dot{\varphi} = 0$ from (14) gives $\alpha^2 = 2n_1 \cot a \cos\varphi$ changing sign with n even or odd. Furthermore, from (12) with $v = \dot{n}_1 = 0$, $n_1 = -N \sin a \cos\varphi$.

Solving the two equations for n_1 and a for a fixed wavenumber of perturbation and plasmon number, the ordered pair

$$\left(n\pi, -\frac{1}{2}N\left[\frac{4N^2\cos^4\varphi - \alpha^4}{N^2\cos^4\varphi}\right]^{1/2}\cos\varphi, \pi - \cos^{-1}\left(\frac{1}{2}\frac{\alpha^2}{N\cos^2\varphi}\right)\right)$$

https://doi.org/10.1017/S002237780500423X Published online by Cambridge University Press

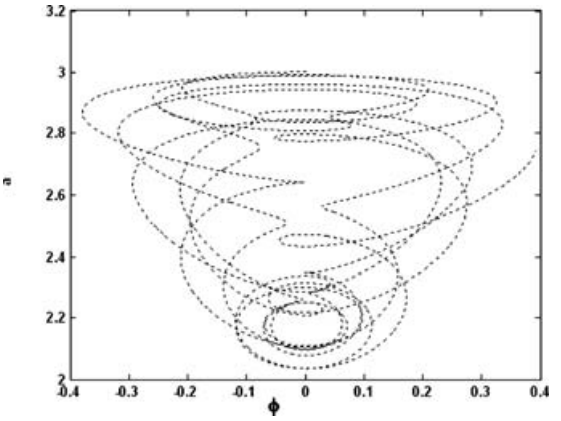

Figure 3. Phase space plot for the Zakharov equations through the simplified model with $A_0 = 1$, $\beta = 0.1$ and $\alpha = 1.2$ showing no FPU recurrence. This behavior is consistent with that obtained in Fig. 1 obtained numerically.

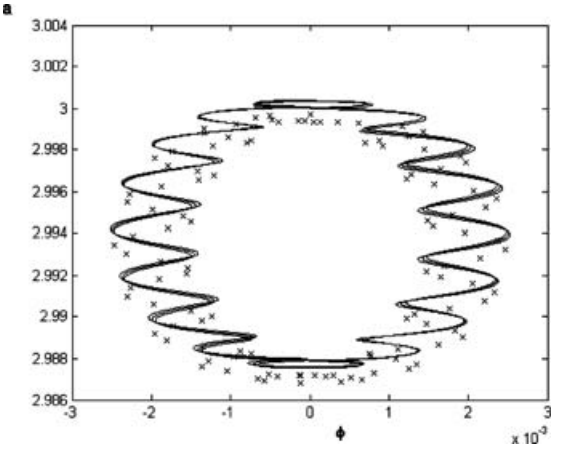

Figure 4. Phase space (a, φ) plot in the adiabatic case when $A_0 = 1$, $\beta = 0.1$ and $\alpha = 1.41$ using the simplified model showing near periodicity consistent with the behavior depicted in Fig. 2, illustrating the presence of a fixed-point attractor. Numerical simulation indicates n_1 oscillates around 0.1480 as also proved analytically in the manuscript. Points on the x-axis are obtained after multiplying by a factor of 10^3. The solid curve is obtained through the simplified model and the dotted points are obtained through the Zakharov model.

defines the equilibrium points or fixed points for the 3D system (φ, n_1, a). The values of n_1 and a, ignoring negative values for n_1 and hence even values of n, can be further simplified and for one value of wavenumber of perturbation the fixed point ($\cos\varphi = 1$) can be defined as

$$\left(2n\pi, \frac{1}{2}N\left[\frac{4N^2 - \alpha^4}{N^2}\right]^{1/2}, \pi - \cos^{-1}\left(\frac{1}{2}\frac{\alpha^2}{N}\right)\right).$$

With initial amplitude $A_0 = 1$, plasmon number $N = 1.005$ and $\alpha = 1.41$ the fixed point is $(2n\pi, 0.1480, 2.9938)$ as illustrated in Fig. 4 where one can view the convergence to this fixed-point attractor in the limit of numerical investigations, also indicating that the system restricts itself to a point in phase space and hence

https://doi.org/10.1017/S002237780500423X Published online by Cambridge University Press

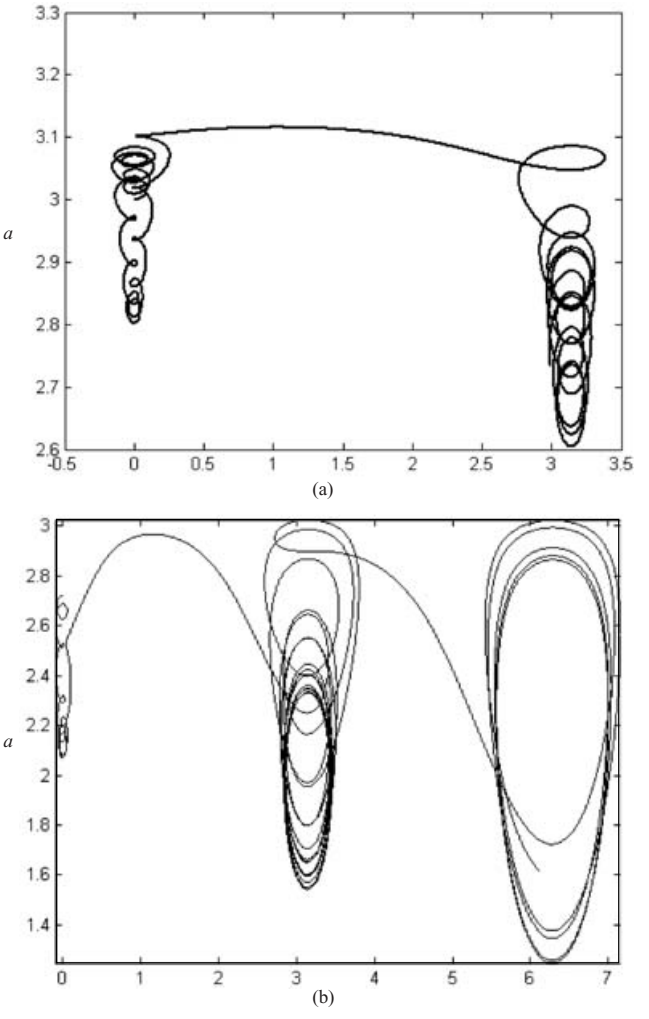

Figure 5. (a) Phase space (a, φ) plot in the non-adiabatic case when $A_0 = 1.0$, $\beta = 0.1$ and $\alpha = 1.42$. Notice a break up of periodicity in the trajectory with a slight increase in the wavenumber of perturbation and (b) when $A_0 = 1.0$, $\beta = 0.5$ and $\alpha = 1.41$ with an increase in the amplitude of perturbation again depicting a break up of periodicity.

an attractor of the system. Deviating the wavenumber of perturbation slightly at initial amplitude $A_0 = 1$ and plasmon number $N = 1.005$ to $\alpha = 1.2$ (refer Fig. 3) the fixed point is $(2n\pi, 0.7012, 2.3695)$.

We introduce four variables f, g, v and q through the following relations

$$f = \dot{a}, \quad g = \dot{\varphi}, \quad v = \dot{n}_1, \quad q = \dot{v} \tag{20}$$

such that on using (12), (13) and (14) the dynamical equations can be written as

$$f = -4n_1 \sin\varphi, \tag{21}$$

$$g = \alpha^2 - 2n_1 \cos\varphi \cot a \tag{22}$$

and

$$\dot{v} + \alpha^2 n_1 = -\alpha^2 N \sin a \cos\varphi \tag{23}$$

https://doi.org/10.1017/S002237780500423X Published online by Cambridge University Press

in a, v, φ, n_1 so that the simplified model can be treated as a four-dimensional (4D) continuous autonomous chaotic system. We will now analyze the basic properties of this system.

From (21)

$$\frac{\partial f}{\partial a} = 0, \quad \frac{\partial f}{\partial v} = 0, \quad \frac{\partial f}{\partial \varphi} = -4n_1 \cos\varphi, \quad \frac{\partial f}{\partial n_1} = -4\sin\varphi.$$

From (22)

$$\frac{\partial g}{\partial a} = 2n_1 \cos\varphi \operatorname{cosec}^2 a, \quad \frac{\partial g}{\partial v} = 0, \quad \frac{\partial g}{\partial n_1} = -2\cos\varphi \cot a, \quad \frac{\partial g}{\partial \varphi} = 2n_1 \sin\varphi \cot a.$$

Similarly, on using (20) and (23) the characteristic equation for the associated stability matrix is given as

$$(1-\lambda)\begin{vmatrix} -\alpha^2 - \lambda & \alpha^2 N \sin a \sin\varphi & -\alpha^2 N \cos a \cos\varphi \\ -2\cos\varphi \cot a & 2n_1 \sin\varphi \cot a - \lambda & 2n_1 \cos\varphi \operatorname{cosec}^2 a \\ -4\sin\varphi & -4n_1 \cos\varphi & -\lambda \end{vmatrix} = 0. \tag{24}$$

The above equation can be solved as

$$(1-\lambda)[-\lambda^3 + \lambda^2 t_1 + \lambda(t_2 + t_3 + t_4) + (t_5 + t_6 + t_7)] = 0 \tag{25}$$

where we introduce variables t_i $(i = 1 \ldots 7)$ through the following equations:

$$t_1 = 2n_1 \sin\varphi \cot a - \alpha^2, \tag{26}$$

$$t_2 = -8n_1^2 \cos^2\varphi \operatorname{cosec}^2 a, \tag{27}$$

$$t_3 = 2n_1 \alpha^2 \sin\varphi \cot a, \tag{28}$$

$$t_4 = \alpha^2 N \sin 2\varphi \cos a, \tag{29}$$

$$t_5 = -8\alpha^2 n_1^2 \cos^2\varphi \operatorname{cosec}^2 a, \tag{30}$$

$$t_6 = -8\alpha^2 n_1 N \cot a \cos a \cos\varphi, \tag{31}$$

$$t_7 = -4\alpha^2 n_1 N \operatorname{cosec} a \sin\varphi \sin 2\varphi. \tag{32}$$

The associated eigenvalues (denoted by S) are

$$S = \begin{bmatrix} 1 \\ \dfrac{C_1^{1/3}}{6} - 6C_2 + \dfrac{t_1}{3} \\ -\dfrac{C_1^{1/3}}{12} + 3C_2 + \dfrac{t_1}{3} + \dfrac{1}{2} i\sqrt{3}\left(\dfrac{C_1^{1/3}}{6} + 6C_2\right) \\ -\dfrac{C_1^{1/3}}{12} + 3C_2 + \dfrac{t_1}{3} - \dfrac{1}{2} i\sqrt{3}\left(\dfrac{C_1^{1/3}}{6} + 6C_2\right) \end{bmatrix} \tag{33}$$

where

$$\begin{aligned} C_1 = {} & 36t_1t_2 + 36t_1t_3 + 36t_1t_4 + 108t_5 + 108t_6 + 108t_7 + 8t_1^3 \\ & + 12\big(54t_1t_3t_6 - 6t_3t_4t_1^2 - 6t_2t_3t_1^2 + 54t_1t_2t_7 + 54t_1t_2t_6 - 72t_2t_3t_4 \\ & + 54t_1t_4t_7 + 54t_1t_4t_6 - 6t_2t_4t_1^2 + 54t_1t_4t_5 + 54t_1t_3t_5 + 54t_1t_2t_5 \\ & + 54t_1t_3t_7 - 36t_2^2t_3 - 36t_2^2t_4 - 3t_2^2t_1^2 - 36t_2t_3^2 - 36t_2t_4^2 - 36t_3^2t_4 \\ & - 3t_3^2t_1^2 - 36t_3t_4^2 - 12t_2^3 - 12t_3^3 - 12t_4^3 - 3t_4^2t_1^2 + 81t_5^2 + 162t_5t_6 \\ & + 162t_5t_7 + 12t_5t_1^3 + 81t_6^2 + 162t_6t_7 + 12t_6t_1^3 + 81t_7^2 + 12t_7t_1^3\big)^{1/2} \end{aligned} \tag{34}$$

https://doi.org/10.1017/S002237780500423X Published online by Cambridge University Press

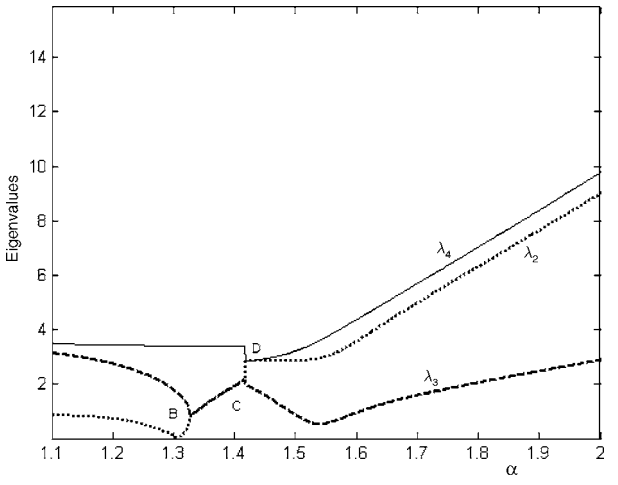

Figure 6. Variation of absolute values of eigenvalues λ_2, λ_3 and λ_4 with wavenumber of perturbation α for the non-adiabatic case.

and

$$C_2 = \left(\frac{-t_2}{3} - \frac{t_3}{3} - \frac{t_4}{4} - \frac{t_1^2}{9}\right) \Big/ C_1^{1/3}. \tag{35}$$

We denote the four eigenvalues by $\lambda_1, \lambda_2, \lambda_3$ and λ_4. The first eigenvalue, $\lambda_1 = 1$ (33) is real and greater than 0. The third and fourth eigenvalues, λ_3 and λ_4 are complex conjugates of each other, indicating the existence of elliptic equilibrium points (see Fig. 4) unstable to slight perturbations (Figs 5(a) and 5(b)). Equation (33) was solved numerically for varied values of the wavenumber of perturbation α. Figure 6 shows the variation of the absolute values of the eigenvalues λ_2 (dotted curve), λ_3 (dashed curved) and λ_4 (solid curve) in the same graph. With specific reference to points B and C in the graph at point B, $\alpha = 1.329(|\lambda_2| = |\lambda_4| = 0.8405)$ and at point C, $\alpha = 1.417(|\lambda_2| = |\lambda_4| = 2.172)$. Beyond point D the eigenvalues are completely distinct. For α values between B and C, λ_2 and λ_4 are complex conjugates of each other, corresponding to the existence of elliptic fixed points as obtained numerically. We also report that the unstable fixed points predict exactly the same growth rate of MI as expected by Zakharov equations in the linear stage [20] justifying the correctness of the model (from the theoretical point of view) in the linear limit.

A second approach to investigate the stability could be to substitute the value of n_1 obtained numerically (for $\alpha = 1.41$, $n_1 = 0.1480$) in (13) and (14) and hence reduce the 4D system to a system of two coupled first-order differential equations. For $\alpha = 1.41$ these equations are

$$v_a(a, \varphi, t) = \dot{a} = 0.592 \sin \varphi \tag{36}$$

and

$$v_\varphi(a, \varphi, t) = \dot{\varphi} = 1.9881 - 0.296 \cot a \cos \varphi. \tag{37}$$

Dividing and eliminating time

$$\frac{da}{d\varphi} = \frac{0.592 \sin \varphi}{1.9881 - 0.296 \cot a \cos \varphi} \tag{38}$$

determines the phase curve with the phase velocity $v(a, \varphi)$.

https://doi.org/10.1017/S002237780500423X Published online by Cambridge University Press

Solving the stability matrix for a system of equations (36) and (37) for eigenvalues yields

$$\lambda^{1,2} = \frac{p_1}{2} \pm \frac{\sqrt{p_1^2 + 4p_2}}{2} \tag{39}$$

where $p_1 = 0.296 \cot a \sin\varphi$ and $p_2 = 0.592 \times 0.296 \cos^2\varphi \operatorname{cosec}^2 a$. For $\varphi = 0$ and for $a > 1$ eigenvalues are complex conjugates of each other with a positive real part and hence the equilibrium points are elliptic fixed points.

Figures 7(a) and 7(b) depict the bifurcation diagram for n_1 iterates with varying values of α for $\beta = 0.1$ and $\beta = 0.2$ with $\varphi_0 = 0$. The behavior remains the same with any initial value of $\varphi_0 = n\pi$. However, the attractor at $\alpha = 1.41$ (Fig. 7(c)) is sensitive to the initial value of $\varphi_0 \neq n\pi$. Figure 8 gives the bifurcation diagram for amplitude a corresponding the bifurcation point at $\alpha = 1.41$.

4.2. Adiabatic case

Using (18) in (16) and (17) we get the following dynamical equations for the adiabatic case:

$$\dot{\varphi} = \alpha^2 + n_0 \cos a(1 + \cos 2\varphi) \tag{40}$$

and

$$\dot{a} = 2n_0 \sin 2\varphi \sin a. \tag{41}$$

Aiming for a determination of fixed points, from (41) $\dot{a} = 0$ implies either that $a = n\pi$ or $\varphi = n\pi/2$ with values of n starting from zero (calling the former as case (a) and the latter as case (b) for future citations in this research paper). For case (a) and case (b) on using (40) with $\dot{\varphi} = 0$ implies

$$\text{for case (a) when } a = n\pi, \quad \varphi = \frac{1}{2}\cos^{-1}\left[-\left(\frac{\alpha^2 + n_0}{n_0}\right)\right], \tag{42}$$

$$\text{for case (b) when } \varphi = n\pi/2, \quad a = \cos^{-1}\left(\frac{-\alpha^2}{2n_0}\right), \tag{43}$$

α and n_0 being positive the argument in (42) would always be greater than one giving complex values of phase φ compared with the argument in (43), which could give real values for a when $\alpha^2 < 2n_0$. Results for case (a) and case (b) are also evident by solving the associated eigenvalue equations with the stability matrices,

$$M_a = \begin{bmatrix} \dfrac{\partial f}{\partial a} & \dfrac{\partial g}{\partial a} \\ \dfrac{\partial f}{\partial \varphi} & \dfrac{\partial g}{\partial \varphi} \end{bmatrix} = \begin{bmatrix} 2n_0 \sin 2\varphi & 0 \\ 0 & -2n_0 \sin 2\varphi \end{bmatrix}, \quad M_b = \begin{bmatrix} 0 & -n_0 \sin a \\ 4n_0 \sin a & 0 \end{bmatrix},$$

with corresponding eigenvalues given as

$$\lambda_{a1} = \pm 2n_0 \sqrt{-\frac{\alpha^2}{n_0}\left(2 + \frac{\alpha^2}{n_0}\right)} \text{ (when } \cos a = +1),$$

$$\lambda_{a2} = \pm 2n_0 \sqrt{-\frac{\alpha^2}{n_0}\left(2 - \frac{\alpha^2}{n_0}\right)} \text{ (when } \cos a = -1)$$

https://doi.org/10.1017/S002237780500423X Published online by Cambridge University Press

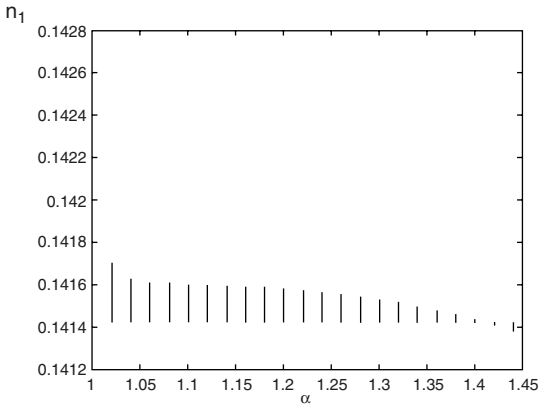

(a)

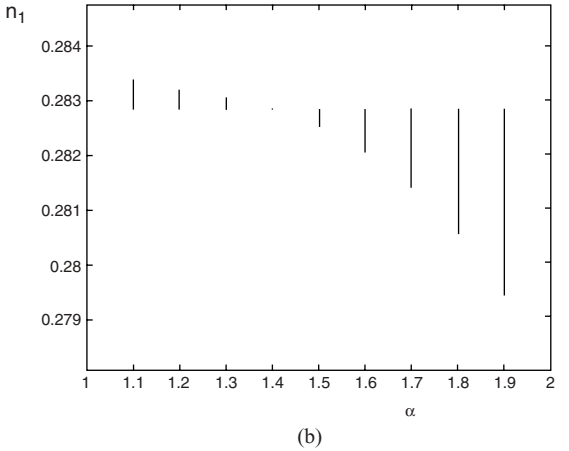

(b)

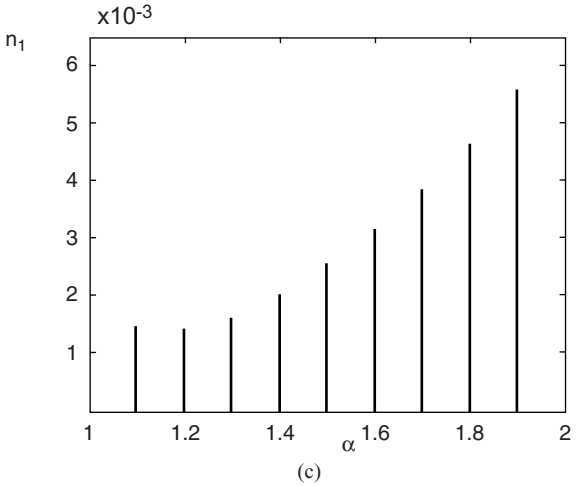

(c)

Figure 7. (a) Bifurcation diagram for $n_1(\alpha \in [1,2])$, $a_0 = 1.0$ and $\beta = 0.1$, $\varphi_0 = 0$. Notice the single value of n_1 near the bifurcation point, (b) $a_0 = 1.0$, $\beta = 0.2$ and $\varphi_0 = 0$. Notice the single value of n_1 near the bifurcation point and (c) $a_0 = 1.0$, $\beta = 0.1$, $\varphi_0 = \pi/2$. Notice the single value of n_1 near the bifurcation point.

https://doi.org/10.1017/S002237780500423X Published online by Cambridge University Press

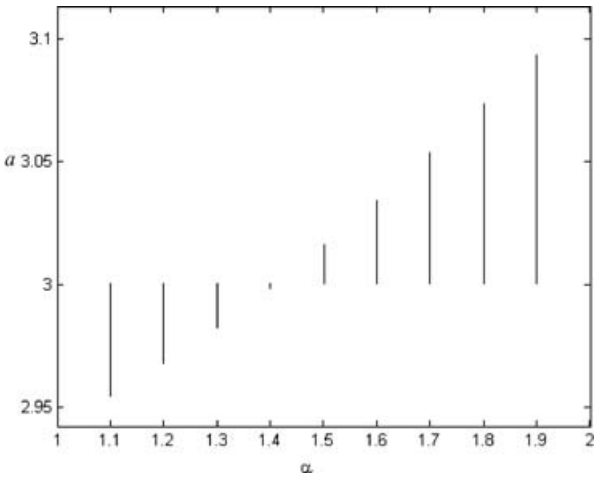

Figure 8. Bifurcation diagram for a ($\alpha \in [1, 2]$), $\beta = 0.1$ and $\varphi_0 = 0$. Notice the convergence to a single value near the bifurcation point.

and

$$\lambda_b = \pm 2n_0 \sqrt{\frac{\alpha^2}{2n_0^2} - 1}.$$

Since the eigenvalues of the stability matrix for case (a) are purely imaginary the fixed points are elliptic. For case (b) with $\alpha = 1.2$, λ_b is again negative demonstrating elliptic fixed points, which is also evident from Figs 9 and 10 with slightly varied values of β (the amplitude of perturbation). One can see the existence of regular orbits is consistent with the results obtained for the NLS case [1, 2, 8–10]. For $\alpha^2 > 2n_0$ roots are real with opposite signs. We could equivalently start simulations with any other value of φ, the nature of stability remaining the same with variations in perturbation wavenumber. Thus, we report that the allowed range of α^2 is given by $0 < \alpha^2 < 2N$.

Corresponding to unstable fixed points, the growth rate of instability γ_I is given by

$$\gamma_I = (-\alpha^4 + 2N\alpha^2)^{1/2} \equiv \gamma_{MI}$$

where γ_{MI} is the linear growth rate of MI as predicted by the NLS equation [1, 2, 8–10], expressed in terms of amplitude.

5. Conclusions

The numerical solutions of the Zakharov equations reveal that nonlinear evolution patterns of MI are quite sensitive to initial conditions. The field in these patterns becomes localized and delocalized but not in a periodic manner as observed in the nonlinear evolution of the 1D NLS equation for the same values of the perturbing wavenumber. We find, in contrast to the NLS equation, the Zakharov equations describe a more realistic evolution of the MI. We define a simplified model for the 1D Zakharov equations that establishes the fact that, as the condition of adiabaticity is relaxed, the FPU recurrence disappears and the chaotic state is observed. The route from the periodic to quasi-periodic to spatiotemporal chaos is studied

https://doi.org/10.1017/S002237780500423X Published online by Cambridge University Press

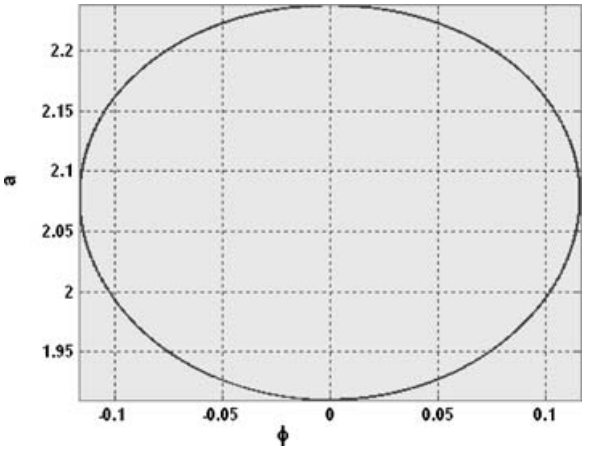

Figure 9. Phase space (a, φ) plot in the adiabatic case when $A_0 = 1$, $\beta = 0.1$ and $\alpha = 1.2$ using the simplified model. Plasmon number $N = 1.005$ (elliptic fixed point in case (b) with complex eigenvalues).

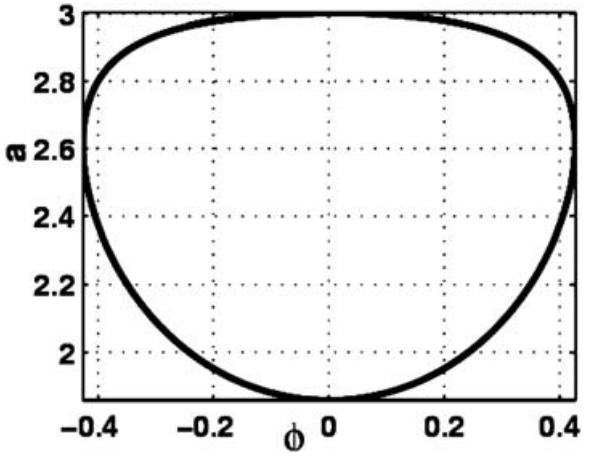

Figure 10. Phase space (a, φ) plot in the adiabatic case when $A_0 = 1$, $\beta = 0.3$ and $\alpha = 1.2$ using the simplified model. Plasmon number $N = 1.0450$ (elliptic fixed point in case (b) with complex eigenvalues).

both numerically and through a simplified model by varying the wavenumber of the perturbation. Results are compared with the numerical results obtained form the Zakharov model. The route from periodic to chaotic behavior is also observable for variations in other input parameters such as β and γ. This research paper further reports the occurrence and the nature of elliptic fixed points (adiabatic case) and a fixed-point attractor (non-adiabatic case where complete FPU recurrence is achieved) for suitable values of wavenumber of perturbation for adiabatic and non-adiabatic cases, respectively. A phase space and bifurcation analysis of the system illustrates that the dynamical system shrinks to a limited volume in phase space for $\alpha = 1.41$, indicating general self-organization leading to a point attractor as is also apparent numerically through the Zakharov model in the same graph.

https://doi.org/10.1017/S002237780500423X Published online by Cambridge University Press

Acknowledgements

This work was initiated when one of the authors (R.P.S.) was visiting the faculty at Equipe Turbulence Plasma (Institut Méditerranéen de Technologie, F-13451 Marseille cedex 13, France) under the European Commission and the Department of Science and Technology, India collaborative project. One of the authors (R.P.S) would specifically like to thank Dr D. F. Escande for the hospitality at IMT and also for useful discussions. This work was partially supported by Department of Science and Technology, India.

References

[1] Yuen, H. C. and Lake, B. M. 1982 *Adv. Appl. Mech.* **22**, 67.
[2] Yuen, H. C. and Fergunson, W. E. 1978 *Phys. Fluids* **21**, 1275.
[3] Anderson, D. 1983 *Phys. Rev.* A **27**(6), 3135.
[4] Sharma, R. P., Stubbe, P. and Verga, A. D. 1996 *J. Geophys. Res.* **101**(A5), 10995–11003 and references therein.
[5] Larroche, O and Pesme, D. 1990 *Phys. Fluids* B **2**(8), 1751.
[6] Adam, J. C., Gourdin SerVeniere, A. and Laval, G. 1982 *Phys. Fluids* **25**(2), 376.
[7] Rozmus, W., Sharma, R. P., Samson, J. C. and Tighe, W. 1987 *Phys. Fluids* **30**(7), 2181.
[8] Infeld, E. 1981 *Phys. Rev. Lett.* **47**, 717.
[9] Moon, H. T. 1990 *Phys. Rev. Lett.* **64**, 412.
[10] Goldstein, P. P. and Rozmus, W. 1990 *Phys. Fluids* B **2**, 44.
[11] Tracy, E. R. and Chen, H. H. 1988 *Phys. Rev.* A **37**, 815.
[12] Zakharov, V. E. 1972 *Zh. Eksp. Teor. Fiz.* **62**, 1745 (Sov. Phys. JETP **35**, 908).
[13] Zakharov, V. E. and Shabat, A. 1971 *Zh. Ekps. Teor. Fiz.* **61**, 118 (Sov. Phys. JETP **34**, 62)
[14] Bhakta, J. C. 1994 *Phys. Rev.* E **49**(1), 667.
[15] Benney, D. J. 1962 *J. Fluid Mech.* **14**, 577.
[16] Bretherton, F. P. 1964 *J. Fluid Mech.* **20**, 457.
[17] Fornberg, B. and Whitham, G. B. 1978 *Philos. Trans. R. Soc. London* **289**, 373.
[18] Gazdag, J. 1976 *J. Comp. Phys.* **20**, 196.
[19] Sharma, R. P., Batra, K. and Verga, A. D. 2005 *Phys. Plasmas* **12**, 1–7.
[20] Shen, M. M. and Nicholson, D. R. 1987 *Phys. Fluids* **30**(4), 1096.
[21] Garnier, J. and Abdullaev, F. Kh. 2000 *Physica* D **145**, 65–83.
[22] Abdullaev, F. Kh. and Darmanyan, S. A. 1997 *J. Opt. Soc. Am.* B **14**(1), 27.
[23] Shen, M. M. and Nicholson, D. R. 1987 *Phys. Fluids* **30**(10), 3150.
[24] Shibata, H. 1999 *Physica* A **264**, 226–233.
[25] Guoyuon Q, Shengzhi D, Guanrong C., Zengqiang C. and Zhuzhi Y. 2005 *Chaos, Solitons and Fractals* **23**, 1671–1682.